PASSIVE SOLAR WATER DISTILLATION: OPTIMIZATION THROUGH FIELD TESTING, NUMERICAL MODELLING, AND STATISTICAL ANALYSIS

ANDRIAMANAMPISOA Tsiry Angelos[1], RANDRIANANTENAINA Manampy[1], RAKOTOARISOA Mialitiana[1], CHAPLIN Harry[2], ZIMMERMANN Karl[2], ANDRIANARISON Edouard[1]

[1]*École Supérieure Polytechnique d'Antananarivo, Université d'Antananarivo, Antananarivo, Madagascar*
[2] *Tatirano Enterprise Sociale, Fort-Dauphin, Madagascar*

ABSTRACT

Passive solar distillation systems like the Panorano model offer a solution for producing sweet (desalinated) water in arid regions. This study optimizes solar still performance by modelling heat and water transfer with COMSOL Multiphysics software and validating these results with field experiments using a concrete solar still. Several design parameters were studied: inclination of the still (28° to 32°), thickness of the glass lid cover (2 to 6 mm), relative height between the water surface and lid (-2 cm to +2 cm), and Construction materials (wood, acrylic plastic, concrete, polyester resin). Statistical analysis using the Taguchi method and Principal Component Analysis were used to identify the key variables. The results show that wood is the best performing material thanks to its low thermal conductivity, followed by acrylic plastic. An inclination close to 30°, an intermediate glass thickness (2-5 mm) and a reduced relative height (-2 cm) optimize heat exchange and condensation in the solar still system. The numerical model proved reliable, with a low Mean Squared Error (0.010-0.160) and a high coefficient of determination (R^2= 0.89). A wide range of evaporated water productivities were observed from 1935 to 5688 mL/m²/day with a high standard deviation (1189 mL/m²/day) indicating a strong influence of environmental conditions. Condensed water, on the other hand, showed less variability (standard deviation of 839 mL/m²/day) with values between 1280 and 3779 mL/m²/day. These results offer promising prospects for improving access to drinking water in various environmental contexts.

Keywords: *Passive solar distillation; Drinking water supply; Sustainable Development Goals 6; Evaporated condensed water productivity; Principal Component Analysis; COMSOL numerical modelling,*

---

1. BACKGROUND

Passive Solar Distillation systems use solar thermal energy to convert salty or brackish water into 'sweet' or fresh-water, thereby contributing to water security. Despite the ability to produce drinking water in arid and semiarid regions without a need for complicated membrane processes, their uptake remains limited. Research has shown that the low thermal efficiency of these devices is often associated with design limitations like a reduced absorptive surface, low-conductivity materials, insufficient cooling of the lid (i.e., still cover), and thermal losses [1]. In addition, the performance of passive stills is highly dependent on environmental conditions including fluctuations in solar radiation, ambient temperature, and properties of the water used [2] [3] [4]. The choice of materials is also crucial; composites such as gypsum mixed with polystyrene can improve thermal insulation [5]. However, these materials must first be assessed in terms of durability, cost, and local availability.

The solar still design considered in this study is called the Panorano, being a play of the Malagasy word 'rano' (meaning 'water') and the French word 'paneaux'; together, it means 'water panel'. The Panorano is a single-sloped cascade passive solar still (Figure 1). The lid (i.e., cover) is a transparent glass sheet about one meter squared which allows light (i.e., thermal energy) to pass through. In the 'closed' model of the Panorano, the box is hermetically sealed so that the evaporated steam condenses when it touches the underside of the glass lid, which is slightly cooler than the box's interior temperature due to glass's good thermal conductivity and a convective heat loss on the outside surface of the glass. The condensed water slides down the underside of the lid where it is captured by a tray on the bottom stage. The entire box is supported on a frame at an angle from the ground that should depend partially of the latitude

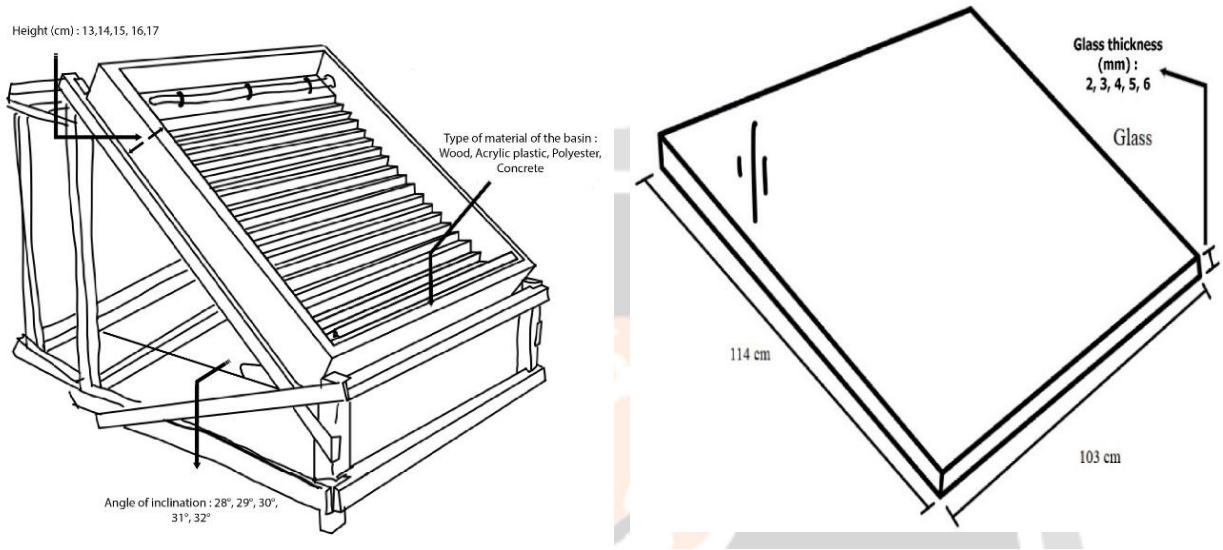

Fig -1. Panorano: a single-sloped cascade style solar still.

of the usage location on the planet to increase solar irradiance capture, but also on keeping the angle steep enough to encourage quick runoff of condensed water.

The present study complements a previous by Randrianantenaina *et al*. who assessed the reliability of a two-dimensional (2D) numerical model of a cascade solar still model called Panorano using COMSOL® Multiphysics [6]. The model simulated the thermal and hydric performances of two physical still prototypes made of concrete or acrylic plastic. The numerical model was based on a multiphysics approach integrating heat transfer (conduction, convection, and radiation), water transport to model evaporation and condensation, and surface-to-surface radiation. The configuration in COMSOL® was:

- **Geometric creation:** A 2D model with layers representing the basin (concrete or plastic), water, moist air, and glass.
- **Definition of materials:** specific properties of the materials used.
- **Boundary conditions:** constant heat flux simulating solar radiation with simplifying assumptions (no vapor leakage and negligible lateral losses).
- **Numerical modelling mesh size:** standard triangular mesh for a balance between accuracy and calculation time.
- **Simulation:** 12-hour period (6am-6pm) with experimental (i.e., field) climate data.

Their results showed that the choice of basin material had a significant influence on the production of distilled water. The acrylic plastic design was modelled to exhibit 4456 mL/m² of evaporation and 2926 mL/m² of distilled water production, compared with the concrete design having 2110 and 1384 mL/m² respectively. The reliability of the model was assessed by comparison with experimental data collected in the summer of 2023 and the winter of 2024. The statistical indicators showed high reliability for the acrylic model in summer (Mean Square Error or MSE= 16.2; R^2 = 0.95) but low reliability for concrete (MSE = 71.5; R^2 = -0.25). In winter, the reliability fell sharply for both materials modelled (negative R^2) because of simplifying assumptions and climatic variability. Limitations were identified as insufficient number of measurements, failure to consider lateral losses or vapour leaks, considering condensation being

limited to glass surfaces, and insufficiently captured seasonal variability. These previous findings highlighted the need to:

- Confirm the reliability of the observed performances,
- Identify and correct specific anomalies, particularly those associated with melted plastic,
- Further optimize design parameters such as inclination, glass thickness, relative pane height, and types of materials used.

The objective of this study was to improve robustness of the solar still numerical model with reproducibility of the observed performances under various testing conditions. This study explores how variations in the design parameters influence the productivity of passive solar water stills by expanding upon a COMSOL Multiphysics numerical model developed originally by Randrianantenaina *et al.* [6]. An approach based on experimental design and statistical analysis was used to identify the optimum configurations for improving the productivity and energy efficiency of the system. By combining numerical modelling and systematic analysis, recommendations are derived to optimize the design of passive solar water stills. These results are intended to increase their efficiency, reduce their limitations, and encourage their use in various contexts, especially in the Androy region of southern Madagascar.

2. LITERATURE REVIEW

This review examines the use of COMSOL Multiphysics in modeling solar water stills and evaluates the parameter estimation methods employed by previous studies. It is a simulation software that uses the finite element method (FEM) to model and solve complex multiphysics problems, where multiple physical processes interact. It supports numerical modeling in areas like structural mechanics, heat transfer, fluid dynamics, electromagnetics, and chemical engineering, with seamless coupling of different physics domains.

2.1. Numerical Modeling and Optimization of Solar Stills Using COMSOL: Opportunities and Challenges

Modelling of solar distillation systems, which should be thought as “energy systems”, involves solving partial differential equations representing the thermal and hydraulic processes occurring within the stills. Numerical simulations using COMSOL software have proven useful for modelling some solar distillation parameters such as glass lid thickness and the integration of phase-change materials, which directly impact system efficiency and productivity [7][8][9]. Additionally, numerical models have enabled the analysis of heat and mass transfer mechanisms including conduction, convection, and radiation, under dynamic environmental conditions involving solar radiation, ambient temperature, and wind speed [10][11][12]. For instance, increased solar radiation was shown to enhance evaporation efficiency, while wind speed presents paradoxical effects by facilitating external cooling but potentially reducing internal thermal stability [13][14][15].

Modeling tools like COMSOL enable the simulation of thermal and hydrodynamic behaviors to assess design and operating factors like surface inclination (i.e., angle of incidence to the sun), material properties, solar intensity, and condensation-evaporation mechanisms [17][18][19]. Furthermore, they enable testing the integration of innovative technologies like nanomaterials and heat recovery systems to maximize productivity while minimizing energy consumption and environmental impact [20][21][22].

Despite their advantages, numerical simulations face obstacles regarding model accuracy and reliability. The multiphysics complexity of modeling solar stills requires coupling thermal, mechanical, fluidic, and electrical phenomena. Simplifying models while maintaining accuracy demands experimental validation, while meshing quality significantly affects simulation convergence and precision. Adaptive meshing techniques are often necessary for areas with steep gradients. Despite these challenges, COMSOL remains an essential tool for advancing solar still development by providing a robust framework for accurate simulations and design validation, paving the way for future innovations in energy systems that enable the production of safe drinking water [23][24].

2.2. Methodologies for Parameter Estimation and Optimization in Solar Still Systems

Mathematical models are developed to predict the thermal processes influencing solar distillation productivity by comparing experimental results with theoretical predictions, enabling model refinement and improved accuracy. Statistical techniques like analysis of variance further enhance the reliability of parameter estimation by quantifying the impact of different factors on system performance and clarifying the relationships between variables [25][26][27]. Full factorial design is a comprehensive experimental method to evaluate the influence of multiple factors on energy

system performance. By testing all combinations of factor levels, this approach provides an exhaustive analysis of individual and combined effects. For example, in heat exchangers, it allows for the simultaneous evaluation of temperature, flow rate, and geometry on thermal energy exchange. The results are analyzed to identify significant factors, assess interactions, and determine statistical significance. This method is often a critical first step in optimization, [28][29].

Despite its advantages, full factorial design has limitations due to the exponential increase in experiments required as the number of factors under consideration increases. Fractional factorial designs offer a practical alternative by reducing the number of experiments while maintaining an acceptable level of accuracy. These approaches collectively contribute to a deeper understanding of solar still systems and support their optimization for improved energy efficiency and productivity [30].

2.3 Recent findings on single sloped solar still optimization

A number of researchers have carried out studies on optimising single sloped solar still:

- Randrianantenaina *et al.* [6] ont modéliser numériquement un distillateur solaire à simple pente pour optimiser sa productivité. La modélisation a montré que l'utilisation du plastique acrylique pour la construction du bassin offrait une plus grande productivité d'eau condensée, mais que le modèle était peu fiable. Le béton (l'autre matériau de construction étudié) a donc été considéré comme plus optimal.

- The performance of a solar still is influenced by the values of the parameters:
    - Inclination: It depends on the balanced capture of sunlight (which depends on the latitude of the test site on Earth) and on maintaining a sufficient inclination to encourage condensed droplets to leave the surface of the glass. Goshayeshi and Safaei (2020) [38] identified a critical angle of 32.5° depending on the geometry.
    - Glass thickness: Panchal and Patel (2017) [39] showed that thinner glazing favors condensation.
    - Type of material: Thermal properties directly influence the heat transfer. Materials with high thermal conductivity improve the overall efficiency.

3. METHODOLOGY

3.1 Field Testing Methodology

Our previous study [6] highlighted the instability in the performance of the physical prototype of Panorano passive solar water stills made from acrylic. Accordingly, the Field Testing portion of this study used only solar stills made from normal concrete in order to assess its performance and reliability over a longer period, from September to November 2024.

This allowed for incremental adjustment of the design parameters of the numerical models to implement a systematic analysis of the design parameters and a cross-validation of the results obtained by numerical simulations and experiments.

3.2. Optimisation of Design Parameters by Numerical Simulation

Building on the findings of the Field Testing (Section 3.1), an incremental adjustment method was adopted to test 500 combinations of the following four parameters that influence Condensed Water Productivity using a full factorial testing plan developed in Minitab® 18.0 (Table 1).

Table -1. Tested factors with their levels

Factors	Levels tested	Considerations
Inclination	28°, 29°, 30°, 31°, 32°	Maximising solar energy capture, will depend on latitude of testing location and maintain sufficient slope to encourage runoff of condensed droplets.
Glass Thickness	2 mm, 3 mm, 4 mm, 5 mm, 6 mm	Balancing light transmission and thermal insulation.
Height from glazing	-2 cm, -1 cm, 0 cm, +1, and +2 cm	Maximizing condensation while limiting heat loss.

Basin Construction Material	Polyester resin, concrete, acrylic plastic, wood.	Balancing thermal properties, workability, durability, cost, and local availability. • Concrete: Thermally stable and durable. • Wood: Environmentally friendly, locally available, and with low thermal conductivity. • Acrylic plastic: Lightweight with good optical properties. • Polyester resin: Water and heat resistant as a composite material.

3.2. Numerical simulations using COMSOL Multiphysics

Numerical modelling was carried out using COMSOL Multiphysics® to simulate multiphysical phenomena involving heat and mass transfer. The model expanded upon the work of Randrianantenaina [31] and incorporated new experimental data to confirm the reliability of the model by carrying out additional tests

The still materials considered were chosen for their thermal properties and local availability in southern Madagascar. The following characteristics were incorporated into the numerical model (Table 2).

Table -2. Physical characteristics of materials for modelling passive solar stills (Data obtained from COMSOL Multiphysics library, online databases [36], datasheet for polyester resin [37], and from specific literature [32] [35])

Properties	**Concrete**	**Acrylic plastic**	**Wood (pine)**	**Polyester resin** [37]
Density (kg m^{-3})	2300 to 2500	1180	500 to 600 [32]	1200 to 1750
Thermal conductivity (W m^{-1} K^{-1})	1.8 to 2.1	0.19 to 0.25	0.12 to 0.15	0.20
Heat capacity at constant pressure (J kg^{-1} K^{-1})	840 to 1000	1470	2300	1200 [33]
Surface emissivity (-) [34] [35]	0.92 to 0.97	0.94	0.90 to 0.95	0.91 to 0.95

The numerical models were evaluated for accuracy by comparing simulated (i.e., predicted) results to the experimental (i.e., actual) observations from ten field trials using the concrete Panorano model conducted between September to November 2024. The simulated and experimental data were evaluated using **Mean Squared Error (MSE)** to assesses the accuracy and **the Coefficient of Determination (R^2)** to assesss the correlation between the simulated results and experimental observations. The quantities of evaporated and condensed water are the responses analyzed following incremental variations of parameters based on an experimental design within the numerical model.

Further analysis of the simulated results was completed using two other techniques. First, the Taguchi method which is based on orthogonal designs and enabled the assessment of the individual effects of the parameters while minimizing the variability of the results. Second, Principal Component Analysis (PCA) was used to reduce the complexity of the simulated data and highlight the key variables explaining the variability in performance.

4. RESULTS

Data was collected using the numerical models to predict distiller performance and field testing to observe actual distiller performance. The following two sections describe the results of each, followed by an evaluation of the Numerical Model based on its ability to predict the field testing observations.

4.1. Numerical model predictions of distiller performance

Figures 2 and 3 show box plots of the evaporated and condensed water volumes, respectively.

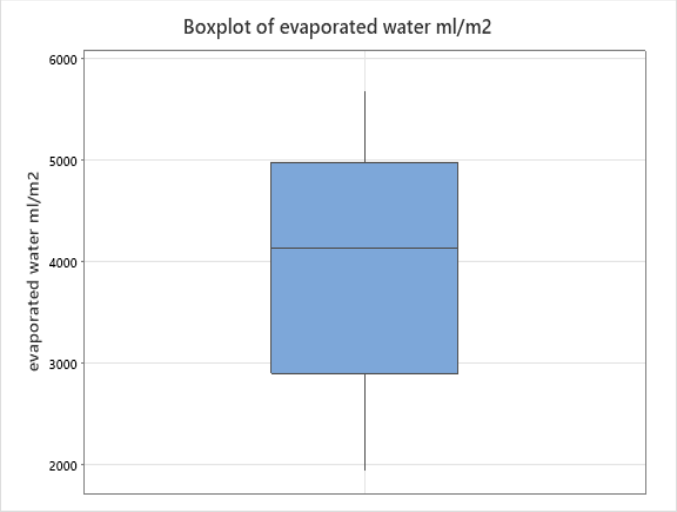

Fig -2: Box plot of evaporated water volumes (mL/m^2)

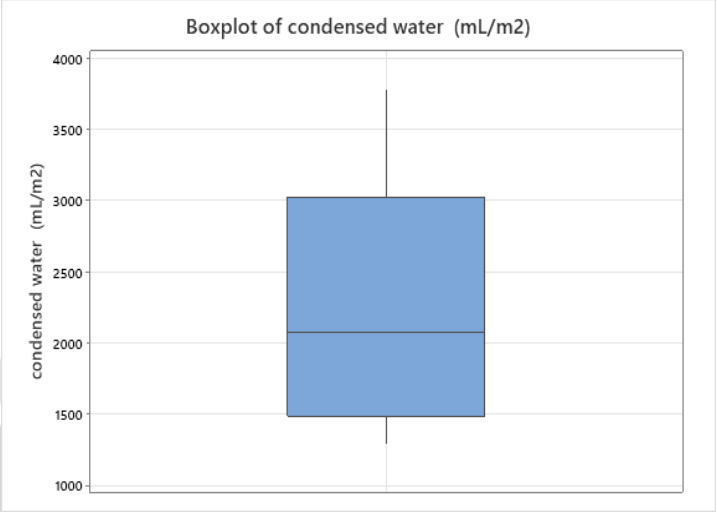

Fig -3: Box plot of condensed water volumes (mL/m²)

The analysis of the boxplots for evaporated and condensed water volumes (mL/m²) reveals distinct differences in data distribution and variability. For evaporated water (Figure 2), the median volume is 4150 mL/m², with 57.5% of observations below this value, while for condensed water (Figure 3), the median is significantly lower at 2150 mL/m², with 42.5% of observations below this value. The interquartile range (IQR) for evaporated water spans 3000 to 5000 mL/m², indicating a moderate spread around the median, whereas the condensed water IQR is narrower, ranging from 1500 to 3000 mL/m², highlighting a more concentrated central distribution. Additionally, the overall data range for evaporated water is 2000 to 6000 mL/m², suggesting relative homogeneity compared to the condensed water range of 1000 to 4000 mL/m², which demonstrates greater variability. These contrasts reflect differences in the processes of evaporation and condensation, with the latter exhibiting a lower median volume and a tighter central dispersion.

A descriptive statistical analysis (Table 3) was performed to identify parameters with the greatest influence on the responses (evaporated et condensed water). The standard deviation of the evaporated water observations was 1,189 mL/m², indicating high variability in the measurements and suggesting that environmental factors strongly influence evaporation, as was also reported in our previous study [6] and elsewhere in literature [40] [41]. The standard deviation for condensed water was lower at 839 mL/m² which suggests a that clean water condensation is less influenced by environmental variations than evaporated water.

Table -3. Descriptive statistics for evaporated and condensed water

Variable	Minimum Value	Maximum Value	Standard Deviation
Evaporated Water (mL/ m^2/day)	1,935	5,688	1,189
Condensed Water collected (mL/m^2/day)	1,280	3,779	839

4.2 Numerical model evaluation using field data

As part of this study, ten measurements were performed on the Panorano experimental device. The results of these measurements were compared to the predictions of the 2D model. The assessment of the reliability of the model is presented in Table 4.

Table -4. Model performance and reliability tests

Field Test No.	Evaluation of Numerical Model performance	
	MSE	**R^2**
1	0.160	0.880
2	0.040	0.760
3	0.010	0.550
4	0.097	0.270
5	0.120	0.330
6	0.020	0.770
7	0.120	0.350
8	0.090	0.300
9	0.030	0.650
10	0.040	0.890
MIN	0.010	0.270
MAX	0.160	0.890
MEAN	0.073	0.073 0.575

Compared to the previous study [6], the verification of the model's reliability in this study was conducted with greater rigor and a larger number of measurements. As shown in Table 4, the model demonstrates a high level of reliability in its predictions, as evidenced by the Mean Squared Error (MSE) and the coefficient of determination (R^2).

- MSE: The values ranged from 0.010 to 0.160, where the minimum value of 0.010 indicates excellent predictive performance, while the maximum value of 0.160 reflects reduced accuracy. Despite this variation, the overall average MSE of 0.073 confirms the model's reliability and its ability to provide acceptable predictions across different scenarios.
- R^2: The coefficient of determination varied between 0.270 and 0.890. A maximum R^2 value of 0.890 indicates that the model explains the variance in the data exceptionally well, whereas a minimum value of 0.270 suggests a weaker fit in certain cases. Nevertheless, an average R^2 value of 0.575 underscores the robustness of the model in capturing key trends and relationships within the data.

Overall, while some individual cases exhibit less optimal performance, the results confirm that the model is globally reliable for producing accurate and meaningful predictions. Notably, with additional measurements, the model's reliability has steadily improved, as reflected by an increase in maximum R^2 from 0.790 in the previous study to 0.890 in this study. This improvement highlights the robustness and accuracy of the proposed model, further validating its applicability for analyzing solar still performance under various conditions.

4.4 Condensed water as a function of Still inclination, Glass thickness, Height, and Construction material

A Taguchi analysis was completed to assess the impact of the tested Parameters (i.e., still inclination, glass thickness, height, and construction material) considering the output response of condensed water collected. Table 5 provides results of the analysis of variance (ANOVA) and Table 6 gives the response table for the signal-to-noise (S/N) ratio; larger S/N ratios are can indicate which input parameters have greater influence out the output responses according to the "Larger is better" approach.

Inclination had no significant effect on S/N ratios ($P = 0.694 > 0.05$). This factor can be considered a secondary or negligible factor to predict condensed water collected. Glass thickness also had no significant effect ($P = 0.450 > 0.05$) on condensed water production. Height, however, had a significant effect ($P = 0.000 < 0.05$) on the S/N ratios. The type of material was the most influential factor, with a highly significant effect ($P = 0.000 < 0.05$). None of the interactions between these Parameters analyzed were statistically significant ($P > 0.05$). Therefore, there was no significant interaction between the factors, and their influence on the condensed water was independent.

The type of construction material had the strongest influence on condensed water collected (Table 6), showing a Delta of 5.87. This was followed in significance by Height with a Delta of 1.38; although its effect is less marked than that

of the type of material, it is still significant. Glass thickness and inclination had low Deltas and limited effects on water condensation in stills.

Table -5: Analysis of variances for S/N ratios (Condensed water).

Source	DF	Seq SS	Adj SS	Adj MS	F	P
Inclination of the still	4	11.870	11.879	2.967	0.560	0.694
Glass thickness	4	19.660	19.660	4.914	0.920	0.450
Height	4	162.220	162.220	40.555	7.620	0.000
Construction material	3	2410.270	2410.270	803.422	150.880	0.000
Inclination of the still * Glass thickness	16	96.100	96.100	6.007	1.110	0.341
Inclination of the still * Height	16	58.610	58.610	3.663	0.680	0.817
Inclination of the still * Construction material	12	44.920	44.920	3.743	0.690	0.759
Residual Error	484	2577.290	2577.290	5.325		
Total	499	5181.300				

Table -6: S/N ratio responses.

Level	Inclination of the still	Glass thickness	Height	Construction Material
1	66.91	66.62	67.28	67.82
2	66.54	66.87	67.07	63.42
3	66.55	66.30	66.83	65.93
4	66.60	66.52	65.90	69.29
5	66.46	66.77	65.97	
Delta	0.44	0.57	1.38	5.87
Rank	4	3	2	1

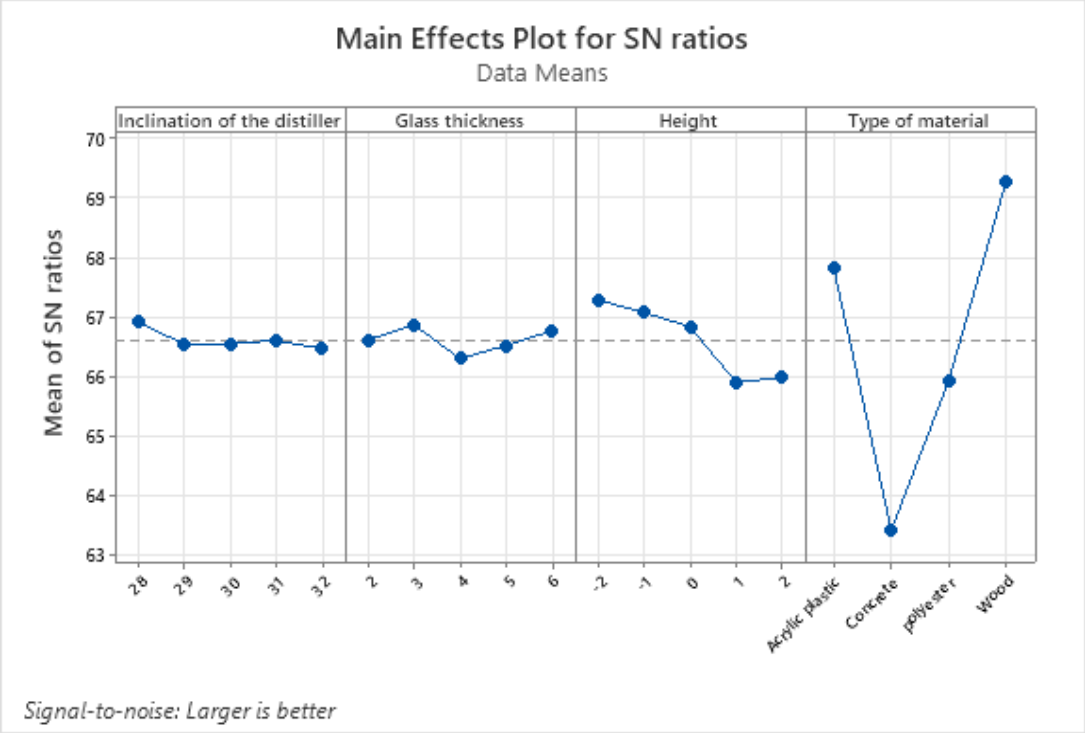

Fig -4: Graphs of main effects for S/N ratios (Condensed water)

Figure 4 shows that the S/N ratios plot for all five Levels of each of the four Parameters. For Inclination had no significant effect since the S/N ratios remained similar at all levels, with a slight peak at 28°. There was a slight variation in the output response for Glass Thicknesses, with the 3 mm level being favorable. However, this variation

is marginal, indicating that Glass Thickness had little impact on the S/N ratios. Height exhibited a significant downward trend: lower heights (-2 cm and -1 cm) produce higher S/N ratios suggesting better performance. The type of Construction Material had the most significant influence on the S/N ratio, with higher ratios for the plastic and wood levels.

The ANOVA for the means (Table 7) were assessed to determine the statistical significance of the effects of the main factors and interactions on the mean response (quantity of condensed water). Inclination (P=0.543>0.05) and Glass thickness (P=0.531>0.05) had no significant effect on amount of condensed water. By contrast, Height (P=0.000<0.05) and Construction material (P=0.000<0.05) were factors that have significant effects. None of the interactions analyzed were significant (P>0.05), indicating that their influences on the quantity of condensed water obtained were independent. Considering the S/N ratio response for the mean response (condensed water), the factor with the greatest influence on the means is the type of material (Delta=1590), followed by the height (Delta=349), then the thickness of the glass (Delta=131), and finally the inclination of the still (Delta=129). The S/N response ratio plots are similar to those in Figure 5 for the output responses, confirming that the Inclination of still has no significant effect on the condensation of water in still. This also shows the negligible effect of Glass thickness and the noticeable effect of Height. Among the factors studied, the Construction material remained the dominant influence to the response. Wood appeared to be the most favorable, followed by plastic.

Table -7: Analysis of variances for Means (Condensed water)

Source	DF	Seq SS	Adj SS	Adj MS	F	P
Inclination of the still	4	1045957	1045957	261489	0.770	0.543
Glass thickness	4	1070404	1070404	267601	0.790	0.531
Height	4	10627498	10627498	2656874	7.860	0.000
Construction material	3	174934506	174934506	58311502	172.450	0.000
Inclination of the still * Glass thickness	16	6367344	6367344	397959	1.160	0.294
Inclination of the still * Height	16	4005528	4005528	250345	0.730	0.761
Inclination of the still * Construction material	12	2826373	2826373	235531	0.690	0.763
Residual Error	484	163653673	163653673	338127		
Total	499	351332037				

Table -8: Response for Means (Condensed water)

Level	Inclination of the still	Glass thickness	Height	Construction material
1	2381	2294	2462	2557
2	2285	2348	2411	1492
3	2265	2217	2349	2037
4	2277	2271	2113	3082
5	2252	2330	2125	
Delta	129	131	349	1590
Rank	4	3	2	1

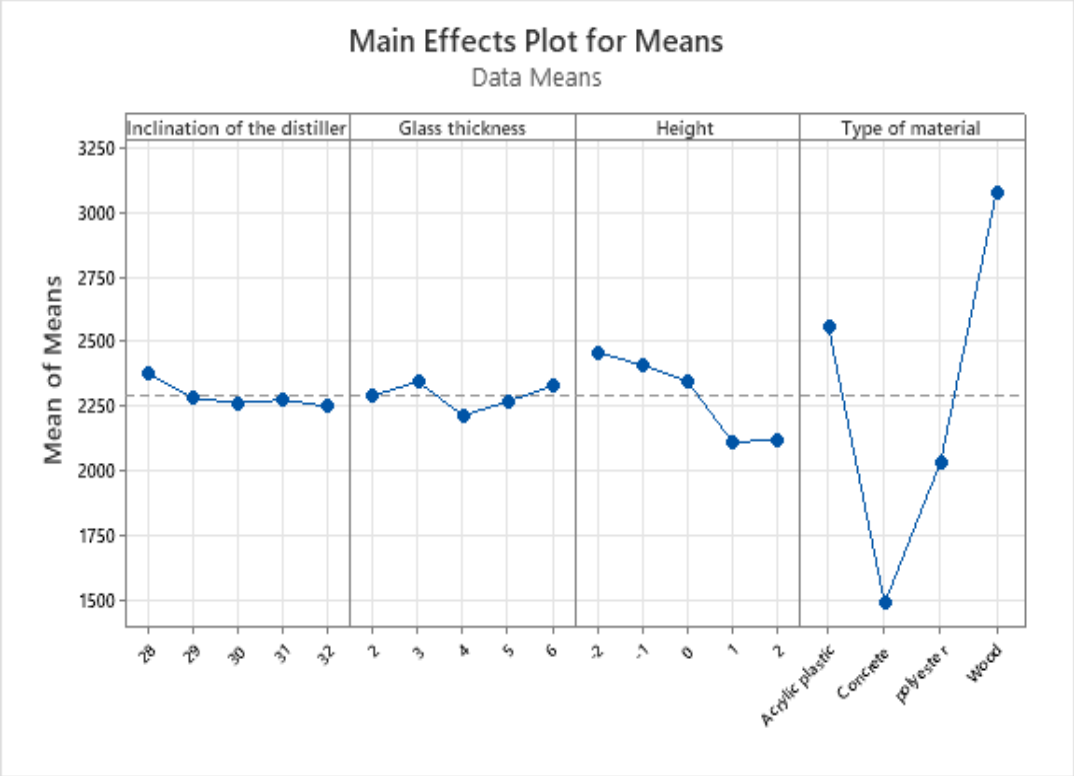

Fig -5: Graphs of main effects for Means (Condensed water)

4.5 Evaporated water as a function of Still inclination, Glass thickness, Height, and Construction material

Similarly, a Taguchi analysis was conducted to assess the impact of the same input Parameters, but this time considering the output response as amount of evaporated water. Table 9 provides the ANOVA results while Table 10 describes the S/N ratio response table and Figure 6 shares the S/N ratios as a response plot.

According to the ANOVA (Table 9), Inclination of the still (P=0.338) and Glass thickness (P=1.000) had insignificant contributions to evaporated water. On the other hand, Height and Construction material (P=0.000) made significant contributions. With a very high value of F (F=4126.55), the type of material had a dominant contribution, underlining its key role. Thus, the interactions between the factors had weak or insignificant contributions.

With a Delta of 7.51, the Construction material is the most influential factor on the evaporated water amount (rank = 1). This was followed by Height (Delta=1.46). Although its effect is less marked than that of the Construction material, it remains significant. Glass thickness and inclination have low deltas and limited effects on water evaporation in the still.

Table -9: Analysis of variances for S/N ratios (Evaporated water)

Source	DF	Seq SS	Adj SS	Adj MS	F	P
Inclination of the still	4	1.450	1.450	0.360	1.140	0.338
Glass thickness	4	0.010	0.010	0.000	0.010	1.000
Height	4	134.760	134.760	33.690	105.570	0.000
Construction material	3	3950.730	3950.730	1316.910	4126.550	0.000
Inclination of the still * Glass thickness	16	3.300	3.300	0.210	0.650	0.846
Inclination of the still * Height	16	4.510	4.510	0.280	0.880	0.588
Inclination of the still * Construction material	12	4.481	4.480	0.370	1.170	0.303
Residual Error	440	140.420	140.420	0.320		

Total	499	4239.661				

Table -10: S/N ratio responses (Larger is better)

Level	**Inclination of the still**	**Glass thickness**	**Height**	**Type of material**
1	71.26	71.30	72.01	72.89
2	71.26	71.30	71.63	67.07
3	71.40	71.30	71.42	70.66
4	71.28	71.31	70.91	74.59
5	71.31	71.30	70.54	
Delta	0.15	0.01	1.46	7.51
Rank	3	4	2	1

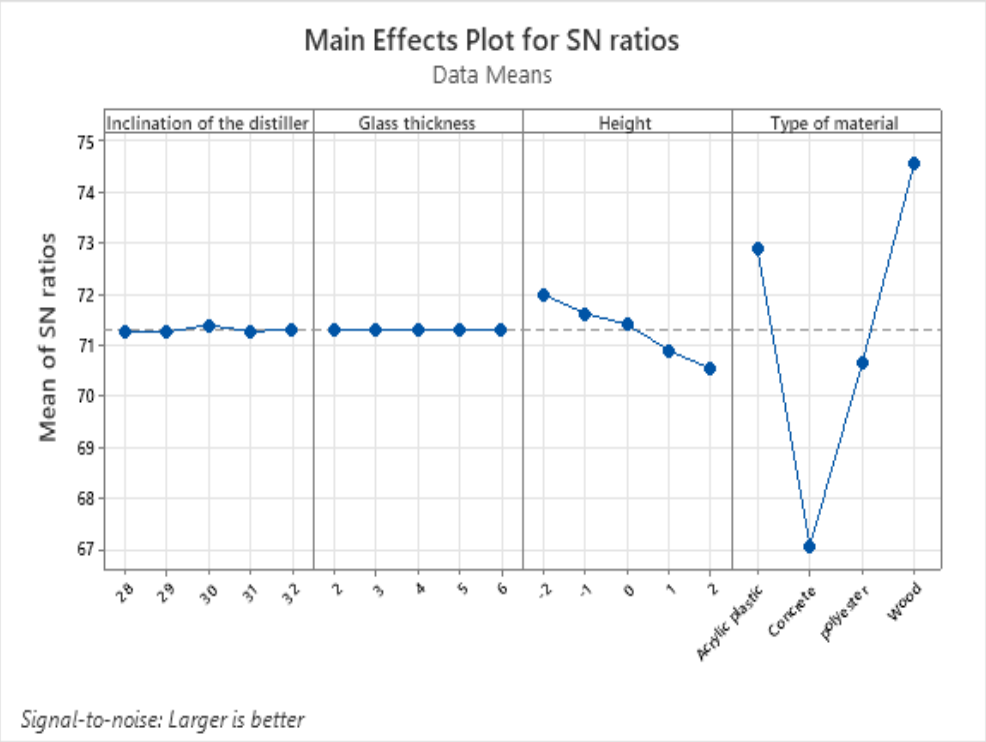

Fig -6: Graphs of main effects for S/N ratios (evaporated water)

Figure 6 shows that the S/N ratios remain constant for all levels of still inclination as well as for all levels of glass thickness. This observation suggests that these two factors have no significant effect on the response. The height shows a decreasing graph, meaning that as this factor increases, the response decreases. The height factor had a significant impact on the response, and its -2 level was the most favorable. As in the previous results, the type of material was the factor that most influenced the response.

Table 11 shows the results of the ANOVA for Means of water evaporation and Table 12 shows the Responses for Means.

Table -11: Analysis of variances for Means (Evaporated water)

Source	**DF**	**Seq SS**	**Adj SS**	**Adj MS**	**F**	**P**
Inclination of the still	4	242681	242681	60670	1.210	0.304
Glass thickness	4	7035	7035	1759	0.040	0.998
Height	4	21442283	21442283	5360571	107.330	0.000
Construction material	3	659281756	659281756	219760585	4400.220	0.000
Inclination of the still * Glass thickness	16	603055	603055	37691	0.750	0.741
Inclination of the still * Height	16	879154	879154	54947	1.090	0.358
Inclination of the still * Construction material	12	597383	597383	49782	0.990	0.456
Residual Error	484	24172454	24172454	49943		

Total	499	705146209				

Neither inclination (P = 0.304 > 0.05) nor Glass thickness (P = 0.993 > 0.05) had a significant effect on evaporation. In contrast, Height (P = 0.000 < 0.05) and Construction material (P = 0.000 < 0.05) were found to have a significant impact. Furthermore, none of the interactions studied were significant (P > 0.05), indicating that their effects on the amount of condensed water obtained were independent.

Table -12: Responses for Means (Evaporated water)

Level	Inclination of the still	Glass thickness	Height	Construction material
1	3867	3874	4158	4415
2	3857	3876	3998	2273
3	3915	3869	3921	3437
4	3855	3878	3714	5366
5	3869	3868	3573	
Delta	60	10	585	3093
Rank	3	4	2	1

Table 12 shows a very large difference between the Deltas of the factors. That of the material type (Delta=3093) far outperforms those of the others, underlining the fact that this factor is the most influential. This was followed by the height (Delta=585) and inclination of the still (Delta=60). The thickness of the glass had a lesser or even negligible impact (Delta =10) on water evaporation.

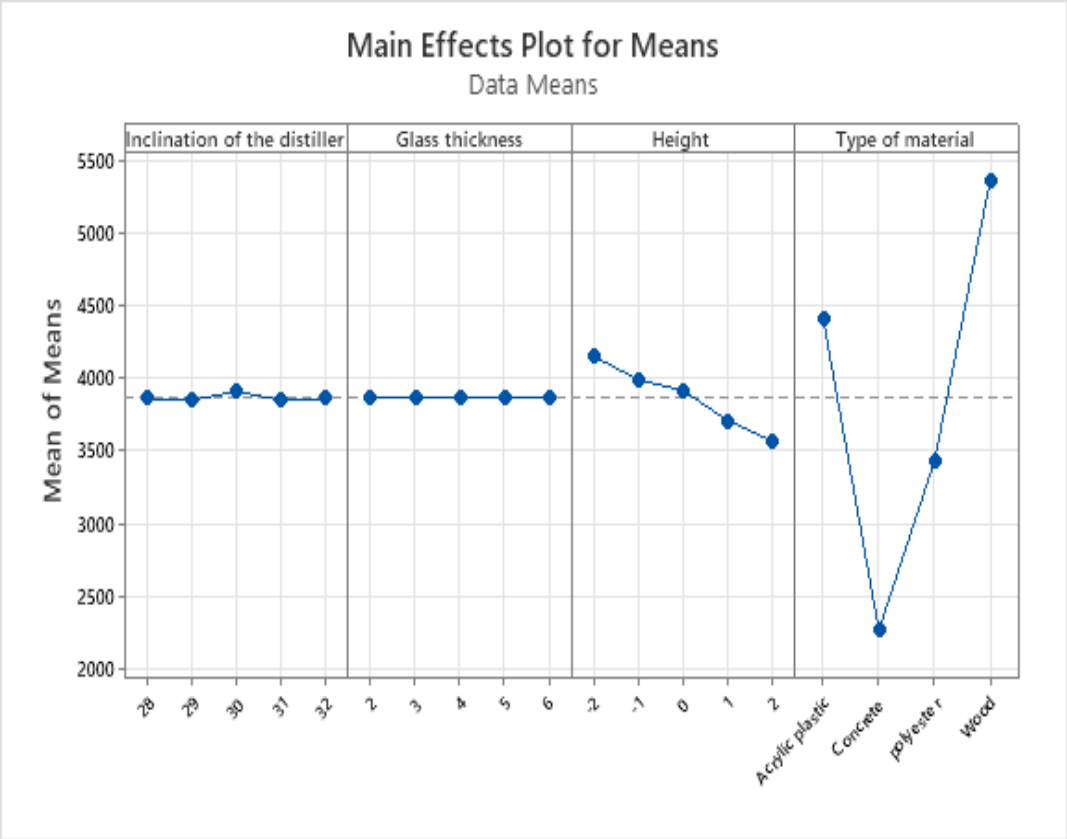

Fig -7: Graphs of main effects for Means (Evaporated water)

The mean responses are constant for all levels of Still inclination as well as for all levels of Glass thickness. This suggests that these two factors have no significant effect on water evaporation. The height shows a decreasing graph, meaning that as this factor increases, the response decreases. The height factor had a significant impact on the response, and its -2 cm level was the most favorable. The large variations in the averages observed according to the type of material indicate that this factor has a significant influence on the response, and that its wood level maximizes it.

4.6. Results of Principal Component Analysis

Principal component analysis (PCA) was used to simplify and identify the key parameters that influence the performance of the solar still. This reduces the dimensionality while retaining the majority of information. Seven input variables were assessed: Inclination of the Still, Glass Thickness, Height, Thermal Conductivity, Surface emissivity, Density, Heat Capacity. Six output variables were also assessed: Evaporated Water, Condensed water, Maximum temperature of air, Maximum temperature of glass lid, Maximum temperature of water inside the box, and Maximum temperature of basin material. Table 13 lists the eigenvalues of the thirteen principal components considered.

Table -13: Eigenvalues of principal components

Variable	PC1	PC2	PC3	PC4	PC5	PC6	PC7	PC8	PC9	PC10	PC11	PC12	PC13
Inclination of the still	0.006	0.007	0.492	-0.853	0.021	-0.089	0.041	-0.075	-0.114	0.003	0.024	0.000	0.000
Glass thickness	-0.002	-0.004	-0.003	-0.027	-0.999	0.003	-0.004	0.006	-0.005	-0.006	0.019	0.000	0.000
Height	-0.016	0.224	0.799	0.489	-0.017	-0.220	-0.005	0.053	-0.058	0.132	0.015	0.000	0.000
Thermal Conductivity	-0.313	-0.361	0.054	0.013	0.006	-0.068	0.430	0.677	-0.152	-0.236	-0.017	-0.001	0.206
Surface emissivity	0.032	-0.855	0.227	0.124	0.000	0.148	-0.305	-0.287	-0.028	-0.047	0.011	0.000	0.038
Density	-0.345	-0.023	-0.035	-0.039	0.006	-0.117	-0.420	0.284	-0.122	-0.028	0.018	0.000	-0.769
Heat Capacity at constant pressure	0.335	-0.148	0.077	0.062	-0.006	0.135	0.661	-0.149	0.101	-0.048	-0.028	0.000	-0.604
Evaporated water	0.344	-0.123	-0.083	-0.036	-0.001	0.102	-0.029	0.313	-0.374	0.776	-0.092	0.001	0.000
Condensed water	0.267	-0.186	-0.185	-0.007	-0.002	-0.925	0.016	-0.060	0.026	-0.009	0.000	0.000	0.000
T° Max (Air)	0.348	0.077	0.031	0.019	-0.003	0.065	-0.155	0.111	-0.254	-0.362	-0.364	-0.710	0.000
T° Max (Glass)	0.349	0.048	-0.009	0.031	0.019	0.077	-0.095	0.137	-0.255	-0.237	0.848	0.003	0.000
T° Max (Water)	0.342	-0.054	0.119	-0.091	0.002	0.074	-0.221	0.450	0.775	0.023	0.002	0.000	0.000
T° Max (Box)	0.348	0.077	0.031	0.019	-0.004	0.065	-0.156	0.112	-0.254	-0.364	-0.370	0.705	0.000

Figures 8, 9, 10, and 11 add more information to Table 13 for precise and rigorous principal component analysis. They show the variation in the eigenvalues of the principal components (Scree Plot, Figure 8), the Mahalanobis distance (Outlier Plot, Figure 9), the distribution of observations in the space defined by the first two principal components (Score Plot, Figure 10), and the projection of the variables onto the first two principal components (Loading Plot, Figure 11).

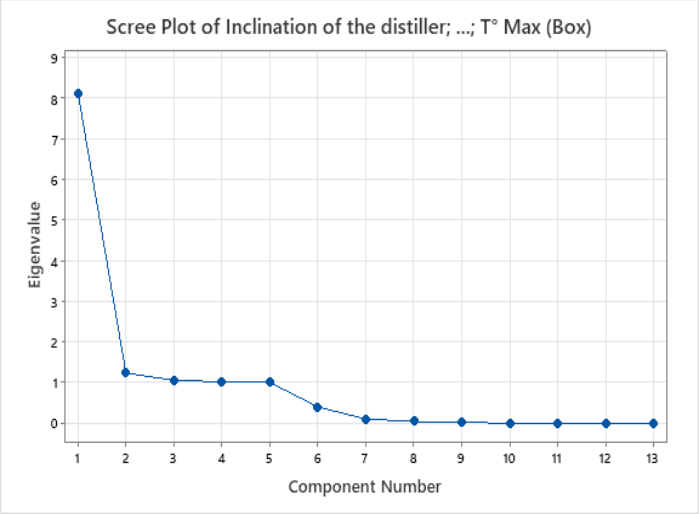

Fig -8: Scree Plot

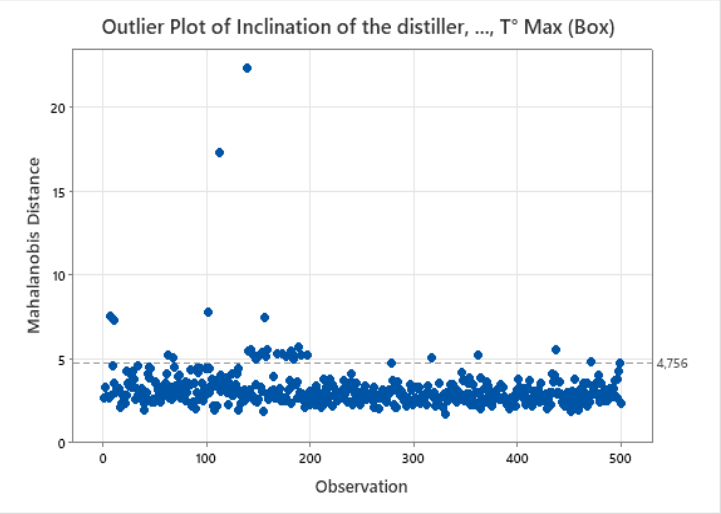

Fig -9: Outlier Plot

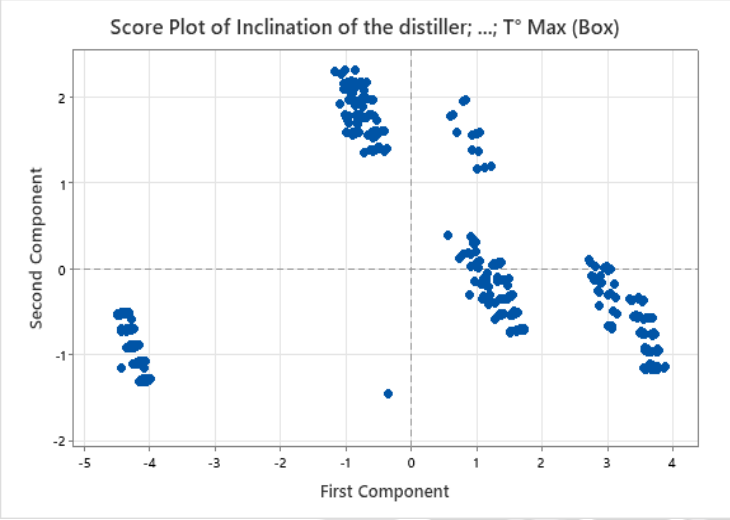

Fig -10: Score Plot

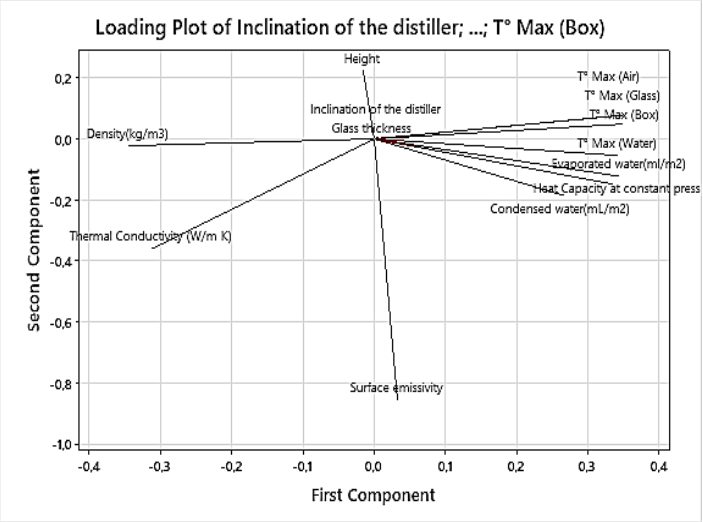

Fig -11: Loading Plot

4.6.1 Scree Plot (Principal Component Analysis)

There was a sharp decrease in the eigenvalues for the first five principal components (PC1 to PC5), which together accounted for 95.7% of the total variance (Figure 8). Therefore, these five components capture most of the information contained in the data, and can be retained to simplify the analysis. They are sufficient to explain almost all the variance in the data.

- The first component (PC1) had an eigenvalue of 8.14 and explains 62.6% of the total variance. According to Table 13, the variables with the highest coefficients were the maximum temperatures (coefficients close to 0.35), condensed water (0.344), and heat capacity (0.335). Therefore, this component was dominated by variables linked to the temperature and thermal performance of the still.
- The second component (PC2) had an eigenvalue of 1.23 and explains 9.5% of the total variance. According to Table 13, the variables with the largest coefficients were surface emissivity (-0.855) and height (0.224). The second component captures the variations linked to the optical and geometric properties of the system.
- The third component (PC3) had a value of 1.06, accounting for 8.1% of the total variance. For this component, according to Table 13, the height (0.799) and inclination of the still (0.492) predominate, suggesting that they reflected the combined effects of the geometric characteristics.

- The fourth component (PC4) explained 7.8% of the total variance and was strongly influenced by the inclination of the still (-0.853).
- The fifth component (PC5) explained 7.7% of the total variance and was strongly associated with glass thickness (0.999).

PCA showed that the system studied is mainly influenced by the maximum temperatures and thermal performance, followed by the optical and geometric characteristics. These variables should be prioritized for interpretation and optimization of the system. A reduction to five dimensions can be envisaged to simplify the analysis, and accounted for 96% of the total variance, suggesting that together these five parameters maintain a representative description of the phenomena studied.

4.6.2. Outlier Plot (Mahalanobis Distance)

The Mahalanobis distance was used to detect outlier observations in a multidimensional space. Observations above the critical threshold (4.756) were considered potential outliers. The majority of observations were below the critical threshold (Figure 9), confirming their alignment with the overall distribution of the data. However, some observations (particularly around indices 50 and 100) exceed the critical threshold with distances greater than 20, which may reflect measurement errors, specific experimental conditions, or rare physical phenomena. An in-depth analysis is required to determine whether they should be excluded or justified. In the cases that they were due to errors or unrepresentative conditions, the values were excluded from subsequent anaylsis. However, if they represented real but rare cases, they remained as included in subsequent analysis, with a specific interpretation.

4.6.3. Score Plot (distribution of observations in the space defined by PC1 and PC2)

Figure 10 shows the spatial distribution of observations defined by the first two principal components (PC1 and PC2). These two components were considered because they explain 62.6 % and 9.5 % of the data. Each point represents an observation and its position in this space is determined by its scores on PC1 (horizontal axis) and PC2 (vertical axis). The observations revealed natural grouping of five distinct clusters, revealing an underlying structure in the data, probably linked to different configurations of the initial variables, such as the inclination of the still or thermal properties. An isolated point near (-1, -2) appears to be an obvious outlier, possibly attributable to an atypical observation or unique experimental condition. The clear separation between the clusters indicates significant differences in the performance or physical characteristics of the studied system.

4.6.4. Loading Plot (Projection of variables on PC1 and PC2)

Figure 11 shows the contributions of the variables to the first two principal components (PC1 and PC2). Each arrow represents a variable and its contribution to the principal components. The arrows represent the variables and their orientation and length indicate their importance and correlation with the components.

- Projections on the horizontal axis (PC1): Maximum temperatures (T° Max (Interior Air, Glass Lid, Water, Basin material)), evaporated water, condensed water, and heat capacity at constant pressure have a strong positive contribution. These variables were highly correlated with each other, suggesting that PC1 was mainly linked to the thermal performance of the system.
- Projections on the vertical axis (PC2): Surface emissivity has a significant negative contribution, whereas height has a positive contribution. This indicates that PC2 captures the variations related to the optical and geometric properties of the system.
- Variables such as the density and thermal conductivity have smaller contributions, suggesting that they play a less important role in the first two dimensions.

5. DISCUSSIONS

This study identified the key parameters influencing the performance of the Panorano passive solar water still. This discussion seeks to interpret these results by aligning them with the study's objectives, comparing them with existing literature, and evaluating their practical implications for optimizing solar still performance.

5.1. Key Design Parameters Influencing Solar Still Performance: Insights from Taguchi Analysis

The results obtained from the Taguchi analysis for both condensed and evaporated water revealed a high degree of similarity in terms of factors influence. Factors exhibit nearly identical effects on the responses. These findings were

further validated and contextualized through comparisons with previous studies, providing a comprehensive understanding of the key parameters affecting solar still performance.

Inclination Angle

Previous studies by Aboulfotoh et al. [42] and Garg and Prakash [43] showed that inclination can significantly impact solar still performance under specific climatic conditions, particularly when the angle is optimized to maximize solar radiation exposure, which should be strongly influenced by the latitude of the testing location to obtain a right angle to the sun's radiation. However, in this study, the influence of inclination was found to be negligible, likely due to the experimental setup, where inclination was not a limiting factor. This may be explained by a qualitative observation during these trials, that while a lesser Inclination should improve solar radiation capture at the testing location (latitude around 25 degrees South at the Field Testing site in southern Madagascar), this effect is complicated by the reduced propensity at lower inclinations for the condensed water droplets to slide down inner glass lid surface. The result was that at lower inclinations, condensed water remained stuck on the lid underside, possibly hindering additional solar radiance from entering the device. As such, we suspect that the optimized inclination must consider both the solar radiation capture, but also maintain a steep enough angle to promote water droplet runoff. For this study, the optimum Inclination was 30°.

GlassThickness

Glass Thickness generally had a limited effect on the overall performance of solar stills. In this study, a moderate glass thickness of 3 mm was identified as optimal, offering a balance between effective transmission of solar irradiance into the device to heat the water, appropriate thermal insulation but also thermal conduction to maintain the underside of the lid as slightly cooler than the air in the Panorano box, so as to promote condensation. This observation is consistent with findings reported in the literature [44].

Height

Height affects the thermal gradient and condensation flux within solar still. Shorter distances between the hot water surface and the cold glass improve heat transfer efficiency by minimizing thermal losses and increasing energy density [45]. The results of this study align with the literature, confirming that reducing the distance between evaporation and condensation surfaces enhances system performance.

Construction Material Selection

Choice of materials for construction is widely regarded as a critical factor in solar still design and performance [46], as well as cost, operability, and durability. In this study, materials like wood and acrylic plastics demonstrated superior performance, which may have been due to their moderate thermal conductivity [47]. These results are in agreement with existing literature, highlighting the importance of selecting appropriate materials to optimize efficiency.

5.2. Application of PCA in Evaluating Solar Still Performance

The findings confirm that PCA is a powerful tool for evaluating the performance of solar stills by reducing data dimensionality while preserving the majority of the information. In this study, five components were found to represent 96% of total variance. These results provide valuable insights into key performance factors.

Thermal Performance as a Key Factor

Maximum temperature emerged as a critical variable influencing the operation of solar stills. Consistent with previous studies [48], the efficiency of solar stills is strongly affected by the temperatures at the water, glass lid, and ambient air. This was reflected in the significant contribution of these variables to the first principal component (PC1), underscoring their importance in optimizing thermal performance.

Influence of Optical and Geometric Properties

Surface emissivity, which governs heat radiation, was a major contributor to the second principal component (PC2). Prior research demonstrated that lowering emissivity can reduce thermal losses through radiation, thereby enhancing overall system efficiency [49]. Additionally, geometric factors such as the height of the still play a crucial role by affecting internal convection and heat transfer. Optimizing this dimension can significantly improve steam condensation and overall productivity.

5.3. Insights from combined Taguchi and PCA Analyses

The findings from the Taguchi and PCA analyses can be summarized as follow:

- **Dominant Factor:** The type of Construction material was identified as the primary factor influencing the performance of the solar still in the Taguchi analysis. This conclusion is further supported by PCA, which highlights that materials directly affect thermal performance through their physical properties, such as thermal conductivity and emissivity. Literature reports also confirm the dominant importance of Construction matieral [50].

- **Secondary Factors:** Height emerged as a significant factor in the Taguchi analysis for maximizing water condensation. PCA provides additional insight by demonstrating that Height indirectly influences performance through its interaction with other thermal parameters, emphasizing its role in optimizing heat transfer and condensation processes. Literature reports highlight the significant effect of the Height on the solar still performance [51].

- **Negligible Factors:** The inclination of the still and the Glass thickness were found to have minimal impact during the Taguchi analysis. This observation is corroborated by PCA, which shows their low contribution to the total variability explained by the model, confirming their limited influence on overall system performance.

5.4. Practical Implications and Limitations of Panorano Model

This study revealed actionable insights towards the implementation of single sloped passive solar water stills as a means of producing sweet water from saline water. Specifically, the use of materials with low thermal conductivity, maintaining a relative distance of approximately 13 cm between the water surface and the glass cover, adopting a top surface inclination angle of 30°, and using a glass thickness of 3 mm are identified as critical design parameters. These recommendations offer a practical framework for improving the efficiency and performance of solar stills. Moreover, the results support the continuing development of numerical models which can be directly employed to minimize the time and resources required for experimental testing. This approach not only accelerates the design process but also enhances its precision by simulating various operational conditions. Additionally, this research underscores the pivotal role of thermal performance in passive solar stills. By integrating these findings into practice, organizations can significantly enhance distilled water production, particularly in arid and semi-arid regions where such solutions are critically needed.

Despite its contributions, this study highlights the limited maximum condensed water collected which was 3779 mL/m²/day. This result underscores the inherently low productivity of passive solar stills compared to equivalent electric-driven desalination setups. This reveals a limitation in their scalability: the passive design is intended to offer simpler operations and maintenance, lower costs, better availability of replacement parts. However, the passive design comes at a detriment to sweet water yield compared to electric desalination system. And so, the passive solar distillation system may only be a preferred option in areas where supply chains to spare parts are challenging or non-existent, trained mechanics and electricians are scarce, and theft of expensive components (like solar panels and motors) may be problematic. This underscores the importance of site-specific considerations when choosing to proceed with a passive or active water production system.

Another notable limitation is the discrepancy between the amount of evaporated water, measured at 5688 mL/m²/day, and the condensed water output measured at 3779 mL/m²/day. This gap indicates substantial inefficiencies in condensed water yield, with the Panorano model exhibiting an inherent performance deficit of 33.5% from its design stage. Such findings emphasize the need for further optimization to reduce inefficiencies and enhance the practical applicability of passive solar stills.

5.5. Future Directions

Future research should develop the Panorano model should foremost focus on improving the condensation and capture of the evaporated water to improve the condensed water yield. This might involve integrating an external condenser unit to improve the capture of evaporated water and enhance both yield and overall productivity. This approach would address the inherent limitations in water production typically observed in passive solar stills. More broadly, the

production constraints of solar distillers should prompt researchers to delve deeper into evaporation-condensation mechanisms across all relevant dimensions, while ensuring usability and accessibility in developing regions.

Another recommendation for future work is to use Construction materials with properties similar to wood or acrylic plastic in terms of thermal insulation, specific heat capacity and emissivity. It may be worthwhile to investigate recycling wood, paper, or plastic wrappers to make new construction materials, reducing the need for harvesting natural wood in areas with deforestation pressures, while integrating a waste valorization approach for a more sustainable solution. Exploring the potential of binder-based paper materials represents a promising avenue for achieving this objective. Such efforts are essential to create scalable, cost-effective, and sustainable solutions tailored to resource-limited environments.

6. CONCLUSION

This study identified critical parameters influencing the performance of passive solar water stills. The findings revealed that height and construction material type are key determinants for maximizing condensation and evaporation, whereas inclination and glass thickness have negligible effects. The study also validated the reliability of a numerical model of the PANORANO passive solar water still by comparing the numerical simulation results and experimental field data, which confirmed the robustness of the model, with mean values of MSE (0.073) and R^2 (0.575) demonstrating its accuracy.

The combined analysis using the Taguchi method and Principal Component Analysis (PCA) further emphasized the dominance of thermal and geometric properties in optimizing system performance. Specifically, it was shown that wood is the optimal material due to its favorable thermal properties, the relative height of the glass should be minimized (-2 mm) to enhance heat transfer and condensation, and a still inclination angle around 30° is recommended, despite its limited influence. Glass thickness, however, was confirmed to have no significant impact on performance and can therefore be freely selected based on other considerations.

These results provide a strong foundation for the development of efficient passive solar stills and contribute to advancing sustainable solutions for addressing water access challenges. By optimizing key design parameters, this study offers practical insights into improving solar distillation systems while promoting environmentally friendly and cost-effective technologies.

7. REFERENCES

[1] V. V. Dongaonkar, S. A. Sable, D. A. Guhe & S. M. Ganorkar (2017), Regenerative Solar Still with Concentrator. *International Journal of Engineering Research and Technology*, Vol. 6, No 04

[2] O. O. Badran (2007), Experimental study of the enhancement parameters on a single slope solar still productivity. *Desalination*, Vol. 209, Issues 1-3, pp 136-143, https://doi.org/10.1016/j.desal.2007.04.022

[3] M. Matouq, A. Tiwary, A. Alaween & J. Othman (2020), Evaluation of a Pilot Saline Water Treatment Unit using a Solar-Thermal Concentrator with Zero Energy Cost for Arid Regions, *Water Productivity Journal*, Vol. 1, No 1, pp 85-92.

[4] T. H. Le, M. T. Pham, H. Hadiyanto, V.V.Pham & A. T. Hoang (2021), Influence of Various Basin Types on Performance of Passive Solar Still: A Review. *International Journal of Renewable Energy Development*, Vol. 10, No 4, pp 789-802, https://doi.org/10.14710/IJRED.2021.38394

[5]. E. T. L. Cöuras Ford, F. A. Ribeiro, R. V. Lima & E. M. Souza (2008), Solar distiller in a pyramidal covering and isolation with composite material. *Revista Engenharia Térmica*, Vol. 7, No 1, pp 37-40, https://doi.org/10.5380/RETERM.V7I1.61739

[6] M. Randrianantenaina, T. A. Andriamanampisoa, M. P. Randrianarison, K. Zimmermann, H. Chaplin & E. Andrianarison (2025), Reliability Analysis of a 2D Model of a Solar Still Developed Using Comsol® Multiphysics, *Open Journal of Modelling and Simulation*, Vol. 13, No 1, pp 20 – 50, https://doi.org/10.4236/ojmsi.2025.131002

[7] O. Guillon (2024), Comsol organise une journée consacrée à la simulation multiphysique et aux énergies renouvelables, *Essais Simulations & Mesures*, [Online] https://essais-simulations-mesures.com/comsol-organise-une-journee-consacree-a-la-simulation-multiphysique-et-aux-energies-renouvelables/, consulted on 18/12/2024

[8] B. N. Shuldes, M. Bavarian & S. Nejati (2021), Multiphysics Modeling and Analysis of a Solar Desalination Process Based on Vacuum Membrane Distillation, *Membranes*, 11, 386, https://doi.org/10.3390/membranes11060386
[9] W. Frei (2023), Modéliser la dispersion dans un modèle de Courants électriques, *COMSOL Blog*, [Online] https://www.comsol.fr/blogs/modeling-dispersion-in-an-electric-currents-model, consulted on 18/12/2024
[10] A. Deliou, B. Khmissi, F. Abdelkader & M. Dehbi (2023), Etude des paramètres et performances d'un distillateur solaire de type chapelle, *1st National Webinar on Process Engineering and Environment (NWPEE'2023)*
[11] N. Bellel & I. Tabet (2012), Etude, réalisation et simulation numérique D'un distillateur solaire à cascade, *Revue des Energies Renouvelables SIENR'12 Ghardaïa*, pp 49 – 57
[12] M. Zerrouki, N. Settou, Y. Marif & M. Benhammou (2014), Simulation numérique d'un distillateur solaire à film capillaire multiétage, Annales de Sciences et Technologie, Vol. 6, No 1, pp 56 – 65, https://doi.org/10.12816/0010628
[13] A. Chaker & G. Menguy (2001), Efficacité interne d'un distillateur solaire sphérique, *Rev. Energ. Ren. : Journées de Thermique*, pp 53 – 58
[14] N. Boukerzaza, A. Chaker, Z. Haddad & B. Benyoucef (2007), Efficacités interne et global d'un distillateur solaire, *13èmes Journées Internationales de Thermique*.
[15] Z. Haddad, A. Chaker & N. Boukerzaza (2007), Etude du couplage d'un distillateur solaire avec un capteur plan, *Revue des Energies Renouvelables* ICRESD-07 Tlemcen, pp179 – 186.
[16] M. Zerrouki, Y. Marif, M. Belhadj & N. E. Settou (2012), Simulation et expérimentation d'un distillateur solaire à film capillaire dans le sud Algérien, Annales des Sciences et Technologies, Vol. 4, No 1, pp 46 – 57.
[17] C. Sonawane, A. J. Alrubaie, H. Panchal, A. J. Chamkha, M. M. Jaber, A. D. Oza, S. Zahmatkesh, D. D. Burduhos-Nergis & D. P. Burduhos-Nergis (2022), Investigation on the Impact of Different Absorber Materials in Solar Still Using CFD Simulation—Economic and Environmental Analysis, Water, 14(19), 3031, https://doi.org/10.3390/w14193031
[18] Q. A. Abed, D. M. Hachim & W. A. Al-Wahid (2021), Performance of cylindrical solar still with hemespherical cover: CFD simulation study, E3S Web of Conferences 286, 02005, https://doi.org/10.1051/e3sconf/202128602005
[19] H. G. Hameed, H. A. N. Diabil & M.A. Al-Moussawi (2023), A numerical investigation of the enhancement of single-slope single-basin solar still productivity, Energy Reports, Vol. 9, pp 484 – 500, https://doi.org/10.1016/j.egyr.2022.11.199
[20] C. Maatki (2023), Numerical Analysis of Entropy Generation in a Double Stage Triangular Solar Still Using CNT-Nanofluid under Double-Diffusive Natural Convection, Mathematics, Vol. 11, No 13, https://doi.org/10.3390/math11132818
[21] J. Mustafa, S. Alqaed & M. Sharifpur (2023), Two phase simulation of solar still in the presence of phase change materials in its bottom and aluminum nanoparticles in the water, Case Studies in Thermal Engineering, Vol. 49, 10335, https://doi.org/10.1016/j.csite.2023.103357
[22] A. Masoumi, M. Jadidi, S. T. Shabestari, M. S. Esmaeili, N. Nazari, M. E. Bidhendi & A. Kasaeian (2024), Enhancing the Performance of a Double Slope Solar Still Employing Nano-Enhanced Phase Change Materials, SSRN, https://dx.doi.org/10.2139/ssrn.4956729
[23] H. O. Ali, A. Khamlichi & H. A. Barkad (2015), Analyse d'un distillateur solaire actif avec récupération de chaleur, *22ème Congrès Français de Mécanique*, Lyon, France.
[24] H. Hafs, A. Zaaoumi, Z. Bouramdane, O. Ansari, A. Bah, M. Asbik & M. Malha (2018), A performance analysis study of a single slope solar still with integrating fins and nanofluids for productivity enhancement, *Proceedings of the 1st International Conference of Computer Science and Renewable Energies (ICCSRE 2018)*, pp 342-348, https://doi.org/10.5220/0009773203420348
[25] V. Modeste, J. L. Rasoanaivo, A. Ravoninjatovo & J. de D. Ramaroson (2022), Conception Et Réalisation D'un Distillateur Solaire En Cascade Avec Appoint, *International Journal of Progressive Sciences and Technologies*, Vol. 36, No. 1, pp. 46-58, https://ijpsat.org/index.php/ijpsat/article/download/4831/2978
[26] A. Deliou, N. Bessas, Z. Belgroun, H. Aburideh, A. Lounis & A. Chikouche (2008), Etude expérimentale des caractéristiques d'un distillateur solaire à effet de serre, *Revues Des Energies Renouvelables CICME 08 Sousse*, pp 109-118
[27]. T. A. Andriamanampisoa, E. N. Andriamanampisoa, K. Zimmermann, H. Chaplin, E. Andrianarison (2024), Identification du modèle de distillateur solaire à effet de serre adapté au Sud de Madagascar : Approche par Matrice de Pugh, *International Journal of Progressive Sciences and Technologies*, Vol 45, N°1, pp 543-564
[28] C. Bassim & B. Lee, Introduction aux méthodes statistiques en ingénierie, [Online] https://ecampusontario.pressbooks.pub/introductionauxmethodesstatistiqueseningenierie/chapter/9-2-1-plans-dexperiences-plans-factoriels-complets/, consulted on 18/12/2024

[29] Plans factoriels et plans factoriels fractionnaires, Assistance de Minitab, [Online] https://support.minitab.com/fr-fr/minitab/help-and-how-to/statistical-modeling/doe/supporting-topics/factorial-and-screening-designs/factorial-and-fractional-factorial-designs/, consulted on 19/12/2024
[30] R. B. Molina, Y. Paradis & L. Salez (2013), Détermination des performances optimales d'un échangeur de chaleur par la méthode des plans d'expériences, *Ecole des Mines de Douai*, Département Energétique Industrielle, Option Génie Energétique
[31] Randrianantenaina, M. (2024), Détermination Et Analyse De La Fiabilité D'un Modèle De Prédiction De Performances D'un Distillateur Solaire : Modélisation 2D Des Paramètres De Conception Sur Le Logiciel Comsol® Multiphysics. Polytechnic Higher School of Antananarivo, *University of Antananativo*
[32] S. Elleuch (2024), Etude des variations des propriétés physiques et chimiques du bois du pin sylvestre (*Pinus sylvestris L.*).[Memoire de Master] , Universite du quebec en Abitibi -Temiscamingue 79p
[33] A. Nouigues (2021), Recyclage des pièces en composite polyester en fibres de verre de grandes dimensions par laminage. Génie mécanique [Thèse de Doctorat]. *Université de Nantes (UN)*
[34] Surface emissivity coefficients, *Engineering ToolBox*, [Online] https://www.engineeringtoolbox.com/emissivity-coefficients-d_447.html , consulted on 19/12/2024
[35] L.Goddijn-Murphy & B. Williamson (2020), Correction: Goddijn-Murphy, L. and Williamson, B. On Thermal Infrared Remote Sensing of Plastic Pollution in Natural Waters. *Remote Sensing*, 2019, *11*, 2159. *Remote Sensing*, Vol. *12*, No 21, 3549. https://doi.org/10.3390/rs12213549
[36] Tableau émissivité en thermodynamique, La librairie thermographique, [Online] https://www.thethermograpiclibrary.org/index.php?title=Tableau_%C3%A9missivit%C3%A9s_en_thermographie , consulted on 19/12/2024
[37] Fiche technique du polyester, Technical Data, [Online] https://www.topglass.com/fr/pultrusion-technologie/caracteristiques-techniques-composites , consulted on 19/12/2024
[38] H. R. Goshayeshi.& M. R. Safaei (2020), Effect of absorber plate surface shape and glass cover inclination angle on the performance of a passive solar still, *International Journal of Numerical Methods for Heat & Fluid Flow*, Vol. 30, No. 6, pp. 3183-3198. https://doi.org/10.1108/HFF-01-2019-0018
[39] H. Panchal, M. I. Patel, B. Patel & R. D. S. Goswami (2011). A comparative analysis of single slope solar still coupled with flat plate collector and passive solar still, *International Journal of Research and Reviews in Applied Sciences*, Vol. 7, pp 111-116.
[40] S. S. S. Al-Mezeini, M. A. Siddiqui, M. Shariq, T. M. Althagafi, I. A. Ahmed, M. Asif, S. J. Alsufyani, Saud A. Algarni, N. Ahamed M.B., K. M. A. Elamin, Abdel-Nasser M. A. Alaghaz & M. M. Gomaa (2023), Design and Experimental Studies on a Single Slope Solar Still for Water Desalination, Water, Vol. 15, No. 4, 704; https://doi.org/10.3390/w15040704
[41] A. N. Olimat, T. A. Rahma, A. S. Awad & A. Alaween (2016), Evaluating Potable Water Production of a Single Slope Solar Still for Waste Water under Jordan Climate Conditions, Journal of Energy Technologies and Policy, Vol.6, No.5
[42] A. M. Aboulfotoh, G. E. Heikal, A. Abdo & Y. G. Khadiga (2023), Solar distillation Systems Design and Enhancements Review, *The Egyptian International Journal of Engineering Sciences and Technology*, Vol. 43, pp 1–18, https://doi.org.10.21608/EIJEST.2022.150949.1178
[43] H.P. Garg & J. Prakash (2000), Solar Energy: Fundamentals and Applications, *Tata McGraw-Hill Education*.
[44] Z. S. Abdel-Rehim & A. Lasheen (2007), Experimental and Theoretical Study of a Solar Desalination System located in Cairo, Egypt, *Desalination*, Vol. 217, No. 1–3, pp. 52–64, https://doi.org/10.1016/j.desal.2007.01.012
[45] A. K. Tiwari & G. N. Tiwari, (2007), Thermal modeling based on solar fraction and experimental study of the annual and seasonal performance of a single slope passive solar still: The effect of water depths, *Desalination*, Vol. 207, No. 1–3, pp. 184–204, https://doi.org/10.1016/j.desal.2006.07.011
[46] H. Panchal, P. Patel, N. Patel & H. Thakkar (2015), Performance analysis of solar still with different energy-absorbing materials, International Journal of Ambient Energy, Vol. 38, No. 3, https://doi.org/10.1080/01430750.2015.1086683
[47] H. Tanaka & Y. Nakatake (2006), Theoretical analysis of a basin type solar still with internal and external reflectors, *Desalination*, Vol. 197, No. 1–3, pp. 205–216. https://doi.org/10.1016/j.desal.2006.01.017
[48] G. N. Tiwari, V. Dimri & A. Chel (2009), Parametric study of an active and passive solar distillation system: Energy and exergy analysis, *Desalination*, Vol. 242, No. 1-3, pp 1 - 18, https://doi.org/10.1016/j.desal.2008.03.027.
[49] A. A. M. Omara, O. E. E. Mohamed, A. A. M. Mohammedali & M. Ahmed (2024), Effect of ten different physical parameters on solar still productivity: Theoretical modeling, *Environmental Progress & Sustainable Energy*. Vol. 43, No. 5, https://doi.org/10.1002/ep.14416

[50] M. Elashmawy, M. M. Z. Ahmed, W. H. Alawee, S. Shanmugan & Z.M. Omara (2024), Scientometric analysis and review of materials affecting solar still performance, Results in Engineering, Vol. 23, https://doi.org/10.1016/j.rineng.2024.102574
[51] M. Roshdy, S. Abdelhady, M. Eissa & M. Esmail (2020), Experimental Measurements on the Effect of Solar Still Basin Height on its Performance, International Journal of Applied Energy Systems, Vol. 2, No. 1, pp 28-32, https://doi.org/10.21608/ijaes.2020.169939